beta-Cell Stress Shapes CTL Immune Recognition of Preproinsulin Signal Peptide by Posttranscriptional Regulation of Endoplasmic Reticulum Aminopeptidase 1

Thomaidou, S.; Kracht, M.J.L.; Slik, A. van der; Laban, S.; Koning, E.J. de; Carlotti, F.; ... ; Zaldumbide, A.

Beta-cell stress shapes CTL immune recognition of preproinsulin signal peptide by post-transcriptional regulation of endoplasmic reticulum aminopeptidase 1

Sofia Thomaidou[1*], Maria J.L. Kracht[1*], Arno van der Slik[1,2], Sandra Laban[2], Eelco J. de Koning[3], Francoise Carlotti[3], Rob C. Hoeben[1], Bart O. Roep[2,4], Arnaud Zaldumbide[1 #]

[1]Department of Cell and Chemical Biology, [2]Department of Immunohematology and Blood Transfusion, [3]Department of Internal Medicine, Leiden University Medical Center, Leiden, The Netherlands, [4]Department of Diabetes Immunology, Diabetes & Metabolism Research Institute, City of Hope, Duarte, USA.

[#] Corresponding author:
Arnaud Zaldumbide, PhD
Department of Cell and Chemical Biology
Leiden University Medical Center
mail stop S1-P, P.O. Box 9600, 2300 RC Leiden, The Netherlands
phone: +31 (0) 71 526 9239 (direct)
E-mail: a.zaldumbide@lumc.nl

[*] **These authors contribute equally to this work**

Keywords: Type 1 diabetes; autoreactive T-cells; miRNA, ERAP1; epitope; processing.

Twitter: ER stress inhibition prevents antigenic peptide presentation and limits beta cell visibility to the immune system. #T1D#JDRF#DON#DFN#INNODIA#LUMC (Figure 4E)

ABSTRACT

The signal peptide of preproinsulin is a major source for HLA class I autoantigen epitopes implicated in CTL-mediated beta-cell destruction in Type 1 Diabetes (T1D). Among them, the 10-mer epitope located at the C-terminal end of the signal peptide was found to be the most prevalent in recent onset T1D patients. While the combined action of signal peptide peptidase and endoplasmic reticulum aminopeptidase 1 (ERAP1) is required for processing of the signal peptide, the mechanisms controlling signal peptide trimming and the contribution of the T1D inflammatory milieu on these mechanisms are unknown. Here, we show in human beta cells that ER stress regulates ERAP1 gene expression at post-transcriptional level via the IRE1α/miR-17-5p axis and demonstrate that inhibition of the IRE1α activity impairs processing of preproinsulin signal peptide antigen and its recognition by specific autoreactive CTLs during inflammation. These results underscore the impact of ER stress in the increased visibility of beta cells to the immune system and position the IRE1α/miR-17 pathway as a central component in beta cell destruction processes and as potential target for the treatment of autoimmune T1D.

INTRODUCTION

Type 1 diabetes (T1D) results from selective and progressive destruction of insulin-producing cells by autoreactive $CD8^+$ T-cells (1; 2). Immunohistochemistry of insulitic pancreases obtained through the Network for Pancreatic Organ Donors with Diabetes program (nPOD) have shown infiltration of immune cells and an increased expression of markers characteristic of the unfolded protein response (UPR) (3))(4-6). Altogether these results suggest an association between endoplasmic reticulum (ER) stress and the increased visibility of beta cells to the immune system (7-9). While several proteins have been identified as potential autoreactive T-cell targets, evidence from both mouse and human studies have suggested that insulin protein itself could be the main and primary autoantigen targeted by infiltrating CD8 T-cells (CTLs) (10-12). The post-translational processing pathway that generates insulin from its precursor molecule preproinsulin (PPI) is well established: the signal peptidase Sec11 cleaves off the signal peptide co-translationally upon translocation of the protein into the ER via the translocon Sec61 (13). After folding and formation of disulfide bonds, proinsulin is transported via the Golgi system into immature secretory vesicles where mature insulin is generated by the combined action of prohormone convertases and release of the C-peptide central region (13-15). Although being the least studied domain of the PPI molecule, increasing evidence highlights the importance of the 24 amino acids long insulin signal peptide (SP) sequence as a major source of insulin derived class I epitopes (16). Peptide elution experiments performed on HLA-A2 purified from surrogate beta-cells have led to the identification of prominent HLA class I binders derived from the signal peptide domain (17) and PPI_{15-24} directed CTLs were found to be highly prevalent in recent onset T1D patients (18). Recently, the importance of the combined action of the signal peptide peptidase and ER aminopeptidase 1 (ERAP1) in the trimming of the PPI signal peptide and in the generation of PPI signal peptide derived epitopes was demonstrated using cell free translocation assay and CRISPR/Cas technology (19). While these data match with the substrate preference of ERAP1 (20; 21), the link between pathophysiological features of T1D and the immunoreactivity against PPI_{15-24} remains unclear.

Here, we investigated the effect of inflammation and ER stress on ERAP1 gene expression in human beta cells and show that proinflammatory cytokines modulate ERAP1 expression both at transcriptional and post-transcriptional level though interaction with miR-17. More importantly, we show in primary human islets that during inflammation the specific inhibition of IRE1a endoribonuclease activity reduces ERAP1 expression and limits signal peptide derived epitope presentation to preproinsulin autoreactive CTLs. Altogether these data establish a direct connection between ER stress and beta cell immunogenicity and

underline the importance of endoplasmic reticulum sensors in shaping antigenic peptide presentation to diabetogenic CTLs.

RESEARCH DESIGN AND METHODS

DNA Constructs

Preproinsulin cDNA was obtained from reverse transcriptase reaction of total human islets RNA extraction using the following primers: *PPI-Full(Fw)*: ATG GCC CTG TGG ATG CGC CTC CTG CCC; *PPI-Full(Rv)*: GTT GCA GTA GTT CTC CAG CTG GTA GAG GGA GCA. LV-CMV-PPI was generated by insertion of the coding region of the preproinsulin cDNA into pLV-CMV-bcGFP. For miRNA reporter construct the following primers were annealed and cloned into pMIR-REPORT (Thermofisher Scientific) open with PmeI. ERAP UTR Fw: 5'-GTA ATT TGA ATA TAG ACA CAA TGC ACT TTA TTG CAC TTT CAA TTC TTA TAA AGC; ERAP UTR Rv 5'-GCT TTA TAA GAA TTG AAA GTG CAA TAA AGT GCA TTG TGT CTA TAT TCA AAT TAC; ERAP UTR mut Fw 5'-GTA ATT TGA ATA TAG ACA CAA TGC ACT TTA TTG TGC TTT CAA TTC TTA TAA AGC; ERAP UTR mut Rv 5'-GCT TTA TAA GAA TTG AAA GCA CAA TAA AGT GCA TTG TGT CTA TAT TCA AAT TAC. The ERAP1 promoter reporter construct was generated by inserting a XhoI/HindIII fragment containing the -1325/+60 region of the ERAP1 promoter into pGL3 vector (Promega). The promoter region was cloned from human genomic DNA using the following primers ERAP prom. Fw: 5'-CCC TCG AGG TCA CAG AAT GAG ATA GAA GGT AGG CAC AAG-3' and ERAP prom Rv: 5'-GGA AGC TTC CTA CCC GCG GCT CGA GCG CGC TGT ACC TGG-3'. The underlined sequences represent the restriction sites used for cloning. The constructs were verified by sequencing.

Cells and reagents

HEK 293T cells were grown in high glucose DMEM supplemented with 10% (v/v) heat inactivated fetal bovine serum (Gibco BRL) and penicillin/streptomycin at 37C, 5%CO2. PPI_{15-24} directed CTLs (17) were maintained in IMDM supplemented with 10% human serum, IL-2 and IL-15 and restimulated every 14 days with irradiated JY cells (pulsed with 2 µg/ml PPI_{15-24} peptide) at 1:1 ratio and irradiated PBMCs of 5 different donors (at a ratio 1:5) in the presence of IL-2, IL-15, Il7, IL12 and leuco-A. PPI_{15-24} was synthesized using solid-phase Fmoc chemistry and analyzed by reverse-phase high-performance liquid chromatography (RP-HPLC), mass spectrometry for purity and identity. HEK293T cells are HLA-A2 positive and routinely used in our lab as target for HLA-A2 restricted CD8 clones (22). Although, many differences could be expected between cell line and primary beta cells, EndoC-βH1 cells remain the best material available to study human beta cell biology (23). EndoC-βH1 cells, obtained from Dr. Raphael Scharfmann (Paris Descartes University, France) (24), were maintained in low glucose DMEM supplemented with 5.5 µg/ml human transferrin, 10 mM Nicotinamide, 6.7 ng/ml Selenit, 50 µM β-mercaptoethanol, 2% human

albumin , 100 units/ml Penicillin and 100 µg/ml streptomycin. Cells were seeded in ECM, fibronectin pre-coated culture plates. Inflammatory stress was induced by a mixture of 1000 U/ml IFNγ and 2 ng/ml IL1β for 24 h. Staurosporine was used at 100nM for 1h and Thapsigargin was used at 100nM for 24h. MKC3946 inhibitor was used at 10uM for 24h in our assay, unless differently stated. The inhibitor was added simultaneously to other treatments.

miRNA and DNA transfection

Transient transfection of miRNA mimics and DNA vectors were performed using Lipofectamine 2000 (Invitrogen) according to manufacturer's protocol. EndoC-βH1 cells were transfected in a 12-well plate, using a final concentration of 200 nM total miRNA precursor. Hsa-miR-17-5p precursor (PM12412, Ambion),pre-miR #1 (negative control 1, AM17110, Ambion) and hsa-miR-17-5p inhibitor (AM12412,Ambion) were used. Experiments were continued 24 h post transfection. For the validation of miRNA targeting sites, 293T cells were cotransfected in a 96-well plate with 125 ng pMiR-luc-ERAP1-wtUTR or pMIR-luc-ERAP1-mutUTR and 50 nM miRNA precursor hsa-miR-17-5p precursor or premiR Hsa-miR-1 per well. Transfections were performed in triplicate and cells were analysed 24 hours post transfection. For the evaluation of ERAP1 transcriptional regulation, EndoC-βH1 cells were co-transfected with the ERAP1 promoter reporter construct and a lentiviral vector including a GFP gene under the control of a cytomegalovirus promoter (CMV) in order to estimate transfection efficiency. Transfections were performed in a 96 well plate with 150ng of total DNA per well. 24 hours later, transfected cells were treated with thapsigargin (100nM) or 1000 U/ml IFNγ and 2 ng/ml IL1β for 24h and luciferase activity was measured.

Luciferase assay

Cells were lysed in luciferase lysis buffer [125 mM Tris/HCl, pH 7.8, 10 mM CDTA, 10 mM DTT, 50% (v/v) glycerol, 5% (v/v) Triton X-100]. Luciferase activity was determined by luminometry using the Promega Luciferase Assay Reagent (Promega, Madison, WI). β-Galactosidase activity was determined by luminometry using the galactolight dual light kit (Tropix). Light emission was determined using Lumat LB9501 luminometer (Berthold, Bad Wildbad, Germany).

Lentiviruses production and transduction

The vectors were produced as described previously(25). Briefly, the lentiviral backbone containing the gene of interest and the three helper plasmids (encoding HIV-1 gag–pol, HIV-1 rev, and the VSV-G

envelope protein) were co-transfected overnight using the calcium phosphate method into 293T cells. The medium was refreshed and viruses were harvested after 48 and 72 h, passed through 0.45-µm filters, and stored at -80°C. Virus was quantified by antigen capture ELISA measuring HIV p24 levels (ZeptoMetrix Corp., New York, NY, USA) as described(26). Then, viral supernatants were added to fresh medium supplemented with 8 mg/ml Polybrene (Sigma), and the cells were incubated overnight. The next day, the medium was replaced with fresh medium. Transduction efficiency was analyzed 3 to 6 days post transduction.

ERAP1 downregulation

shRNA lentiviral constructs for ERAP1 knockdown were obtained from the Mission shRNA library (Sigma-Aldrich clones TRCN060539; TRCN060540; TRCN060541; TRCN060542). Based on preliminary assays to assess knock-down efficiency (data not shown), we selected the TRCN060542 clone for further use. shERAP1 encoding lentivirus was produced as described above.

RT-PCR / qPCR

Total RNA was extracted from cultured cells using Trizol reagent following manufacturer's instructions. Isolated RNA was quantified using a Nanodrop 1000 spectrophotometer. Approximately 500 ng RNA was reverse transcribed using Superscript RT II kit (Invitrogen, Karlsruhe, Germany). Expression of the genes interest was detected using the following primers: Insulin Fw GCA GCC TTT GTG AAC CAA CA, Insulin Rv CGG GTC TTG GGT GTG TAG AAG; ERAP1 Fw GAA AAC CAT GAT GAA CAC TTG G, ERAP1 Rv CCA CCT CTT CTG GGA GGA TGA G; GAPDH Fw ACA GTC AGC CGC ATC TTC TT, GAPDH Rv AAT GAA GGG GTC ATT GAT GG, XBP1s Fw 5'-CTG AGT CCG CAG CAG GTG-3', XBP1s Rv 5'-GAG ATG TTC TGG AGG GGT GA-3'; ERAP2 Fw GGG GCT TTC CCA GTA GCC ACT AAT GG, ERAP2 Rv GAA TCT TCC TCT GAC TGA AGG GTG GC; Polymerase chain reactions were performed on a PTC-200 (Biozym, Landgraaf, The Netherlands) using the following conditions: 94°C for 5 min; 35 cycles of 30'' at 94°C, 30'' at 60°C, and 1.5 min at 72°C; 10 min at 72°C. Real-time PCR were performed in triplicate using the SybrGreen master mix kit (Applied Biosystems, Nieuwerkerk a/d lJssel, The Netherlands) and an Applied Biosystems Step One Plus. Comparative ΔΔct values were performed using GAPDH gene as reference. Values are represented as mean ± standard error.

Taqman assay

For microRNA quantification, total RNA was reverse transcribed using Taqman microRNA Reverse transcription kit (Applied Biosystems) and detected using Hsa-miR17 Taqman microRNA assays

(PN4427975, Applied Biosystems) and TaqMan 2x Universal PCR Master Mix, no UNG (applied Biosystems) according to manufacturer's instructions. MicroRNA expression was normalized to RNU6 using the following primers: RNU6 Fw 5'-CTC GCT TCG GCA GCA CA-3'; RNU6 Rv 5'-AAC GCT TCA CGA ATT TGC GT-3'.

Western blot analyses

Cells were lysed in buffer containing 50 mM Tris-HCl pH 7.4, 250 mM NaCl, 0.1% Triton X-100, 5 mM EDTA. The lysis buffer was supplemented with protease inhibitor cocktail (Roche). Protein quantification was performed with the BioRad protein assay reagent. For ERAP1 analyses, 50 ug of proteins extracts were loaded on 12% acrylamide/bis acrylamide SDS page gel. After electrophoresis, protein transfer was performed on a nitrocellulose membrane (GE Healthcare). Membranes were stained with anti-ERAP1 overnight at 4 °C (Santa Cruz B10; Sc-271823), goat anti-mouse IgG HRP (Santa Cruz, sc-2005) was used for the detection. Beta actin was used as a loading control (EMD Millipore, MAB1501).

Flow cytometry

For intracellular insulin staining, cells were fixed at 4°C with 2% PFA PBS for 20 min, followed by 10 min incubation at 4°C with permeabilization buffer (0.5% saponine, 2% BSA, PBS). rabbit anti-insulin (Santa Cruz Biotechnology, sc-9168) and anti-rabbit-PE (#111,116,144, Jackson ImmunoResearch, 1:500 dilution) were used. All antibody incubations were performed in the permeabilization buffer for 30 min at 4°C. For surface staining, cells were incubated on at 4°C for 30 min with monoclonal mouse anti-human HLA-ABC Antigen/RPE Clone W6/32 (DAKO, R7000) or with mouse anti-human CD8 APC (BD Pharmigen, 555369) in the flow cytometry buffer (0.5% human albumin, 0.01% Na azide, PBS). Analysis was performed using BD LSR II (BD Biosciences) and Flowjo software. A total of 10.000 events were recorded.

Islet donors

Pancreatic islets were obtained from human organ donor pancreata. Human islets were isolated from organ donors. Islets were only studied if they could not be used for clinical purposes and if research consent had been obtained. According to the national law ethics approval is not required for research on donor tissues that cannot be used for clinical transplantation. The isolations were performed in the GMP-facility of LUMC according to the previously described protocol (27). For experimental use, human islets were maintained in ultra-low attachment plates (Corning, NY 14831) in low glucose DMEM supplemented with 10% FBS, 100 units/ml Penicillin and 100 µg/ml streptomycin. Dispersed islet cells were treated with

1000 U/ml IFNγ, 2 ng/ml IL1βfor 24 hours to induce ER stress. All methods were carried out in accordance with relevant guidelines and regulations.

T cell activation assays

Islet preparations were washed with PBS and dispersed by trypsinization in an ultra-low attachment 6 well plate. The day after cells were counted and seeded in a 96 well plate at a concentration of 50,000 (for donor R153 and 615) or 200,000 (for donor R155) islet cells per well. Treatment with proinflammatory cytokines and MKC3946 was performed as described for 24h. On the third day HLA-A2-PPI 15-24 specific CTLs were added at a ratio 5E: 1T (for donor R153 and 615) or 1E:2T (for donor R155) in presence of mouse anti-human CD107a- FITC (ThermoFisher Scientific, 11-1079-42) was added. Co-cultures were incubated at 37 °C for 2 hours. Cells were washed with flow cytometry buffer (0.5% human albumin, 0.01% Na azide, PBS), stained for CD8 and analysed by flow cytometry, as mentioned above. The absolute degranulation (D) capacity of T cells was calculated as a ratio of [% of CD107a+ cells/ % total CD8+ cells] (data not shown). The relative degranulation was estimated by calculating the % of change of the absolute degranulation of the treated samples compared to their respective controls. More specifically for the cytokine treated sample: $((D_{CYT} - D_{DMSO})/ D_{DMSO})$*100. For the cytokine plus MKC3946 sample: $((D_{CYT} - D_{MKC3946})/ D_{MKC3956})$*100.

The supernatant was used for detection on MIP 1 beta production by the T cells, using the MIP 1 beta ELISA kit (ThermoFisher Scientific, BMS2030INST), according to manufacturer's protocol.

In silico analyses and statistical analysis

miRNA interaction with ERAP1 mRNA have been evaluated by crossing information available at miRbase v21.0 (http://www.mirbase.org/) and Tarbase v.8 (http://carolina.imis.athena-innovation.gr/diana_tools/web/index.php?r=tarbasev8/index) using beta cell specific miRNAs databases published in (28; 29). Venn Diagram was generated using online Ven diagram plotter (https://omics.pnl.gov/software/venn-diagram-plotter).Data are presented as mean ± SEM . Calculations were performed using GraphPad Prism 7. Unpaired t-tests were carried out in all comparisons, except from the experiments of T cell activation upon co-culture with dispersed islets (Figure 4E,F), where a paired t-test between samples of the same islet donor was performed ($p>0.05$:ns/ $p \leq 0.05$: */ $p \leq 0.01$: **/ $p \leq 0.001$: ***/ $p \leq 0.0001$:****).

Data resource and availability. The datasets generated during and/or analysed during the current study are available from the corresponding author upon reasonable request.

RESULTS

ERAP1 is required for PPI signal peptide antigen processing

The localization of insulin signal peptide within the ER and the TAP (Transporter associated with antigen processing) independent routing of the PPI_{15-24} have suggested proteasome independent degradation mechanisms (17). The presence of three alanine residues at the C-terminal part of the insulin signal peptide represents a high-affinity binding motif for the hydrophobic pocket of ERAP1 and the two leucine residues in position 13-14 makes this region a suitable substrate for ERAP1 trimming (Figure 1A) (20; 30). To test for the implication of ERAP1 on preproinsulin signal peptide processing and to evaluate the consequences for antigenic peptide recognition by CTLs, surrogate beta cells were generated by genetically modifying HEK 293T cells with a lentiviral vector containing the full-length preproinsulin cDNA, driven by a CMV early enhancer and promoter. After verification of the increased insulin gene expression in these cells (Figure 1B), we used an ERAP1 directed shRNA containing lentivirus to specifically downregulate ERAP1 gene expression. Transduction of ERAP1 shRNA (MOI=1) led to 90% reduction in ERAP1 mRNA level compared to non-target control shRNA (Figure 1C). Interestingly, in these experiments ERAP1 downregulation increased significantly ERAP2 gene expression (Figure 1D) but had no impact on (pro)insulin expression or HLA class I surface expression (Figure 1E-F). Yet, co-culture of modified cells with PPI_{15-24}-specific, HLA-A0201-restricted CD8 T-cells showed a reduced T-cell activation as measured by T-cell degranulation (exposure of CD107a at the cell surface) (Figure 1E) and a reduced MIP1β secretion (Figure 1F). These data support the role of ERAP1 in the processing of the PPI_{15-24} epitope from human PPI (14).

ERAP1 is upregulated by inflammation and Endoplasmic Reticulum stress

In the course of diabetes development, proinflammatory cytokines secreted by infiltrating immune cells are believed to promote autoimmunity by inducing ER stress in beta cells (7; 31-33). In order to evaluate the impact of T1D pathophysiological condition on ERAP1 gene expression, EndoC-βH1 cells were exposed to a mixture of proinflammatory cytokines (i.e., IFNγ and Il-1β) or to Sarcoplasmic reticulum Ca^{2+}-ATPase (SERCA) pump blocker (i.e., thapsigargin) as ER stress inducer. Although the stress response of EndoCBH1 and primary human beta cells differs (34), cytokine treatment and thapsigargin stimulation led to increase expression of marker from the unfolded protein response (UPR) in EndoCBH1 (Supplementary figure S1 and S2). In these conditions, the increased stress status as measured by XBP1 splicing (Figure 2A), correlated with an upregulation of ERAP1 expression both at gene and protein level (Figure 2B-C). In order

to characterize the underlying regulatory mechanisms, we generated a luciferase reporter construct to assess the transcriptional regulation of the ERAP1 gene by introducing the ERAP1 promoter region (-1325/+60) (35) upstream a luciferase encoding sequence (Figure 2D). Following transfection of the reporter construct in EndoC-βH1 and stress treatment induction, a 3-fold increase in light emission after IFNɣ/IL1β treatment was observed, which confirms the transcriptional regulation by IFNɣ (36). However, the absence of transcriptional activation of the ERAP1 promoter after thapsigargin treatment in our assay, suggested additional regulatory mechanisms controlling ERAP1 gene expression during ER stress.

miR17-5p acts as a post-transcriptional regulator of ERAP1 expression

To evaluate a possible post-transcriptional control of ERAP1 mRNA by micro RNAs (miRNAs), we searched for potential miRNA binding sites within the ERAP1 3'-UTR region. Using beta cell specific miRNA datasets (37) and two different algorithms for prediction of miRNA binding sites (miRbase and TarBase (28; 38)) (Supplementary table 1), six putative miRNAs were identified that could be expressed by beta cells and destabilize ERAP1 mRNA expression (Table 1 and Figure 2E). Notably, these miRNAs belong to the miR-17 family, implying a conserved mechanism of regulation. To confirm these *in silico* findings, luciferase reporter constructs were generated harboring a 54 nucleotides long fragment of the ERAP1-3'UTR carrying the predicted miR-17 binding site as well as a mutant construct containing two nucleotides substitution preventing the formation of the miRNA-induced silencing complex. Transient transfection of miR-17 in HEK293T luciferase reporter cells reduced luciferase activity from the native UTR reporter construct but had no effect on the luciferase mutant construct (Figure 2F). To validate that miR-17 expression negatively affects ERAP1 mRNA in beta cells, we forced expression of miR-17 in EndoC-βH1 and determined ERAP1 gene expression by qPCR. Transient transfection of miR-17 resulted in 30% reduction of ERAP1 gene expression while co-transfection of the complementary anti-miRNA (anti-miR-17) reversed the inhibitory effect of miR-17 on ERAP1 gene expression (Figure 2G). Of note, insulin gene expression in these assays remained stable (Figure 2H). Altogether, these results reveal that miR-17 contributes to ERAP1 regulation by direct interaction with the ERAP1 3'-UTR region. To connect inflammation induced ER stress and miRNA regulation, EndoC-βH1 cells were treated with cytokines and miR-17 expression was determined by Taqman assay. Consistently with previous reports (39), we observed over 20% decrease in miR-17 expression after 24hours treatment, indicating that these cytokines may modulate ERAP1 expression by affecting miR-17 level (Figure 2I). These results have been confirmed after chemical induced stress by thapsigargin (Supplementary figure S2B). In line with these

results, transfection of miR-17 in EndoC-βH1 blunted proinflammatory cytokine induction of ERAP1 (Figure 2J) without affecting insulin gene expression (Figure 2K).

IRE1α inhibition partially restores ERAP1 homeostatic expression

Previous studies have identified miR-17 as an important link between the endoribonuclease IRE1α and the induction of beta cell death via activation of the thioredoxin-interacting protein (TXNIP) (39). To determine whether the ERAP1 post-transcriptional regulation in stress conditions was mediated by IRE1α, EndoC-βH1 beta-cells were treated with cytokines and XBPs, miR-17 and ERAP1 gene expressions were followed for 24h in a time course experiment (Supplementary figure 2A). As anticipated, IFNγ/IL1β stimulation led to decreased expression of miR-17 and increased expression of both XBPs and ERAP1. Interestingly, specific inhibition of IRE1α, by MKC3946 treatment (40), increased expression of miR-17 both at 6h and 24h in homeostatic condition and prevented its degradation in cytokine conditions (Figure 3A, 3C). Under these conditions, cytokines induced ERAP1 gene expression was partially reduced by MKC3946 co-treatment at 6h (Figure 3B). This observation was more pronounced after 24h treatment where inhibition of the cytokine induced ERAP1 gene expression reached 40% (Figure 3D) without any effect on cells viability (supplementary Figure S3A). IRE1α inhibitor dose response experiments performed in EndoC-βH1 illustrated the direct correlation between IRE1α activity (as assessed by spliced XBP1 expression) and ERAP1 gene expression (Figure 3E-F). Chemical induced stress led to similar changes in gene expression (Supplementary figure S2B), also in these conditions, the effect of thapsigargin on ERAP1 expression was inhibited by MKC3946 cotreatment (Supplementary Figure S2C). More importantly, similar experiments performed in freshly isolated human islets confirmed that the increased ERAP1 expression mediated by cytokines or thapsigargin could be counteracted by MKC3946 treatment (Figure 4 A-B).

IRE1α inhibition limits PPI signal peptide epitope presentation to autoreactive specific CTLs

In order to determine the consequences of our findings on the insulin signal peptide trimming, presentation and subsequent CTLs activation, we examined whether IRE1α inhibition affects immune recognition of the $PPI_{15–24}$ signal peptide derived epitope presented by primary human beta cells. Following dispersion, isolated human islet cells (HLA-A2) were maintained for 24h in presence or absence of IFNγ/IL1β and treated with MKC3946. After treatment, islet cells were co-cultured with the PPI_{15-24} -specific, HLA-A0201-restricted CD8 T-cell clone for 2 hours prior to the analyses (Figure 4C). We verified that MKC3946 had no deleterious effect on T-cell function, no direct effect on CD107a surface expression (Supplementary figure S3B, S3C, S3D) and no effect on HLA class I surface expression on islet cells (Figure

4D) and determined T cell activation in the different conditions by measuring T-cell degranulation and MIP1β secretion. We demonstrated in islet preparations from three different pancreas donors that CD107a surface expression in CD8 positive cells was significantly increased after coculture with islet cells treated with cytokines, illustrating an increased surface density of the specific peptide HLA ligand at the beta cell surface. Furthermore, we showed that MKC3946 cotreatment abrogates the deleterious effect of cytokines on T cell degranulation (Figure 4E). Quantification of the MIP1β production in the cell supernatant confirmed the effect of the IRE1α inhibition on PPI_{15-24} peptide processing (Figure 4F), supporting the notion that ER stress is involved in shaping CTL responses in T1D.

DISCUSSION

We demonstrate that ERAP1 is critical for the generation of a prevalent preproinsulin-derived autoantigenic peptide, and present a new regulatory mechanism connecting ER stress and increased beta cell visibility to the immune system.

The upregulated ERAP1 expression observed both in isolated human islets and in a human beta cell line after cytokine stimulation or chemically-induced stress extend proof for the implication of ERAP1 in PPI signal peptide processing/presentation (19) and its participation in beta cell destruction during inflammation in T1D patients. Several Leucine amino peptidases induced by interferon-gamma have been shown to participate in peptide trimming(41), however few have been shown to be located specifically within the endoplasmic reticulum, where processing of the insulin signal peptide is likely to occur. Without excluding the participation of other ER resident endopeptidases to the process the reduced T-cell activation and degranulation of PPI_{15-24} CTL observed after coculture with ERAP1 knock-down surrogate beta cells or human islet cells treated with the IRE1α inhibitor is in line with a previous study targeting ERAP1 expression by specific siRNA (19). Yet, it remains to be established whether the observed reduction in T cell activation is sufficient for protecting beta cells from CTLs mediated attack. Similarly to previous study (42), the reduced expression of ERAP1 led to increased expression of ERAP2 in our assays. On the view of the complementarity role of these two aminopeptidases (43), this compensatory effect may explain the absence of effect of the ERAP1 knock-down on HLA class I surface expression. Similar experiments performed in human and mouse cells have shown a maximal 10% reduction after ERAP1 downregulation by siRNA (44; 45). Though the effect of the ER stress inhibitor on adhesion and costimulatory molecules has not been studied in depth, the lack of effect of MKC3946 on HLA-A/B/C expression in human islet cells suggests that the differential T cell activation observed is a direct consequence of the relative density of PPI_{15-24}/HLA complexes at the cell surface.

ERAP1 has been initially described as IFNγ responsive gene (46). Although we cannot exclude the presence of ER stress responsive element in enhancer region more upstream to the promoter core region chosen in our transcriptional based assays, our results are pointing to two distinct regulatory mechanisms during inflammation: a transcriptional regulation mediated by IFNγ responsive elements (i.e. IRF1 binding sites) within the ERAP1 promoter proximal region, and an ER stress-dependent post-transcriptional regulation. In fact, our data using the SERCA pump blocker thapsigargin show additional regulatory mechanisms of ERAP1, initiated by the ER stress sensor IRE1α and involving a post-transcriptional control of ERAP1 mRNA. The results obtained in human islet cells exposed to IRE1α inhibitor where MKC3946 treatment

completely abolishes the chemically-induced ER stress mediated ERAP1 expression but only partially impacts (~50%) cytokine-induced expression, perfectly illustrate this dual regulation.

Several miRNAs have been implicated in the response to stress (47); Among these, miR-17 has been shown to be a master regulator of beta cell apoptosis by controlling the thioredoxin-interacting protein for T1D and T2D (39; 48). Interestingly, TXNIP regulation was demonstrated to be dependent of both PERK and IRE1α sensors (49). The incomplete downregulation of ERAP1 in our experiments after treatment with MKC3946 inhibitor may also implies that, as for TXNIP, multiple arms of the UPR could be involved in ERAP1 regulation.

In this study, we confirmed the complexity of antigenic peptide generation originating from signal peptide domain of the human preproinsulin. The implication of the IRE1α/miR-17 pathway in regulating the resident ER protein trimming underscores the key role played by ER stress in the development of autoimmunity. We propose that inflammatory cytokines released by infiltrating autoreactive immune cells during insulitis increase beta cell visibility to the immune system by increasing peptide processing and presentation (increase HLA). The increased density of PPI_{15-24} peptide-HLA complex at the beta cell surface would be the consequence of a combined direct transcriptional activation mediated by binding of interferon regulatory factors to the ERAP1 promoter and post-transcriptional control of the ERAP1 mRNA mediated by the IRE1a/miR-17 axis (Figure 4G). Supported by recent work performed in NOD mice highlighting the potential of IRE1a kinase inhibitors in maintaining beta cells integrity and preserving beta cell function(50), our study designates IRE1a as a relevant therapeutic target to reduce beta cell visibility to the immune system and to prevent T cell-mediated destruction in human diabetes pathogenesis.

Acknowledgments

The authors want to thank Steve Cramer (CCB) and Martijn Rabelink (CCB) for technical help.

Fundings

This work is supported by JDRF, DON and the Dutch Diabetes Research Foundation and by the IMI2-JU under grant agreement No 115797 (INNODIA). This Joint Undertaking receives support from the Union's Horizon 2020 research and innovation program and "EFPIA", 'JDRF" and "The Leona M. and Harry B. Helmsley Charitable Trust". BOR is supported by the Wanek Family Project for Type 1 Diabetes.

Author Contributions: S.T. and M.J.L.K. performed the experiments and wrote the manuscript, A.S. and S.L. performed the experiments, F.C. and E.J.P.K provided with human islets and wrote manuscript; R.C.H. wrote the manuscript, B.O.R., AZ supervised the project, designed the experiments and wrote the manuscript. AZ is the guarantor of this work and, as such, had full access to all the data in the study and takes responsibility for the integrity of the data and the accuracy of the data analysis.

Competing interest: No potential conflicts of interest relative to this work are reported.

REFERENCES

1. Bottazzo GF, al-Sakkaf L, Dean BM, Schwarz G, Pujol-Borrell R: [Hypotheses on the etiology of insulin-dependent diabetes: published and recent ideas]. Journ Annu Diabetol Hotel Dieu 1985:135-147
2. In't Veld P, Lievens D, De Grijse J, Ling Z, Van der Auwera B, Pipeleers-Marichal M, Gorus F, Pipeleers D: Screening for insulitis in adult autoantibody-positive organ donors. Diabetes 2007;56:2400-2404
3. Campbell-Thompson M, Wasserfall C, Kaddis J, Albanese-O'Neill A, Staeva T, Nierras C, Moraski J, Rowe P, Gianani R, Eisenbarth G, Crawford J, Schatz D, Pugliese A, Atkinson M: Network for Pancreatic Organ Donors with Diabetes (nPOD): developing a tissue biobank for type 1 diabetes. Diabetes Metab Res Rev 2012;28:608-617
4. Campbell-Thompson M: Organ donor specimens: What can they tell us about type 1 diabetes? Pediatr Diabetes 2015;16:320-330
5. Marhfour I, Lopez XM, Lefkaditis D, Salmon I, Allagnat F, Richardson SJ, Morgan NG, Eizirik DL: Expression of endoplasmic reticulum stress markers in the islets of patients with type 1 diabetes. Diabetologia 2012;55:2417-2420
6. Richardson SJ, Willcox A, Bone AJ, Morgan NG, Foulis AK: Immunopathology of the human pancreas in type-I diabetes. Semin Immunopathol 2011;33:9-21
7. Marre ML, Piganelli JD: Environmental Factors Contribute to beta Cell Endoplasmic Reticulum Stress and Neo-Antigen Formation in Type 1 Diabetes. Front Endocrinol (Lausanne) 2017;8:262
8. Kracht MJ, van Lummel M, Nikolic T, Joosten AM, Laban S, van der Slik AR, van Veelen PA, Carlotti F, de Koning EJ, Hoeben RC, Zaldumbide A, Roep BO: Autoimmunity against a defective ribosomal insulin gene product in type 1 diabetes. Nat Med 2017;23:501-507
9. Kracht MJL, Zaldumbide A, Roep BO: Neoantigens and Microenvironment in Type 1 Diabetes: Lessons from Antitumor Immunity. Trends Endocrinol Metab 2016;27:353-362
10. Kent SC, Chen Y, Bregoli L, Clemmings SM, Kenyon NS, Ricordi C, Hering BJ, Hafler DA: Expanded T cells from pancreatic lymph nodes of type 1 diabetic subjects recognize an insulin epitope. Nature 2005;435:224-228
11. Nakayama M, Abiru N, Moriyama H, Babaya N, Liu E, Miao D, Yu L, Wegmann DR, Hutton JC, Elliott JF, Eisenbarth GS: Prime role for an insulin epitope in the development of type 1 diabetes in NOD mice. Nature 2005;435:220-223
12. Zhang L, Nakayama M, Eisenbarth GS: Insulin as an autoantigen in NOD/human diabetes. Curr Opin Immunol 2008;20:111-118
13. Liu M, Wright J, Guo H, Xiong Y, Arvan P: Proinsulin entry and transit through the endoplasmic reticulum in pancreatic beta cells. Vitam Horm 2014;95:35-62
14. Chang SG, Choi KD, Jang SH, Shin HC: Role of disulfide bonds in the structure and activity of human insulin. Mol Cells 2003;16:323-330
15. Huang XF, Arvan P: Intracellular transport of proinsulin in pancreatic beta-cells. Structural maturation probed by disulfide accessibility. J Biol Chem 1995;270:20417-20423
16. Abreu JR, Martina S, Verrijn Stuart AA, Fillie YE, Franken KL, Drijfhout JW, Roep BO: CD8 T cell autoreactivity to preproinsulin epitopes with very low human leucocyte antigen class I binding affinity. Clin Exp Immunol 2012;170:57-65
17. Skowera A, Ellis RJ, Varela-Calvino R, Arif S, Huang GC, Van-Krinks C, Zaremba A, Rackham C, Allen JS, Tree TI, Zhao M, Dayan CM, Sewell AK, Unger WW, Drijfhout JW, Ossendorp F, Roep BO, Peakman M: CTLs are targeted to kill beta cells in patients with type 1 diabetes through recognition of a glucose-regulated preproinsulin epitope. J Clin Invest 2008;118:3390-3402

18. Velthuis JH, Unger WW, Abreu JR, Duinkerken G, Franken K, Peakman M, Bakker AH, Reker-Hadrup S, Keymeulen B, Drijfhout JW, Schumacher TN, Roep BO: Simultaneous detection of circulating autoreactive CD8+ T-cells specific for different islet cell-associated epitopes using combinatorial MHC multimers. Diabetes 2010;59:1721-1730
19. Kronenberg-Versteeg D, Eichmann M, Russell MA, de Ru A, Hehn B, Yusuf N, van Veelen PA, Richardson SJ, Morgan NG, Lemberg MK, Peakman M: Molecular Pathways for Immune Recognition of Preproinsulin Signal Peptide in Type 1 Diabetes. Diabetes 2018;67:687-696
20. Chang SC, Momburg F, Bhutani N, Goldberg AL: The ER aminopeptidase, ERAP1, trims precursors to lengths of MHC class I peptides by a "molecular ruler" mechanism. Proc Natl Acad Sci U S A 2005;102:17107-17112
21. Evnouchidou I, Momburg F, Papakyriakou A, Chroni A, Leondiadis L, Chang SC, Goldberg AL, Stratikos E: The internal sequence of the peptide-substrate determines its N-terminus trimming by ERAP1. PLoS One 2008;3:e3658
22. Hoyng SA, Gnavi S, de Winter F, Eggers R, Ozawa T, Zaldumbide A, Hoeben RC, Malessy MJ, Verhaagen J: Developing a potentially immunologically inert tetracycline-regulatable viral vector for gene therapy in the peripheral nerve. Gene Ther 2014;21:549-557
23. Tsonkova VG, Sand FW, Wolf XA, Grunnet LG, Kirstine Ringgaard A, Ingvorsen C, Winkel L, Kalisz M, Dalgaard K, Bruun C, Fels JJ, Helgstrand C, Hastrup S, Oberg FK, Vernet E, Sandrini MPB, Shaw AC, Jessen C, Gronborg M, Hald J, Willenbrock H, Madsen D, Wernersson R, Hansson L, Jensen JN, Plesner A, Alanentalo T, Petersen MBK, Grapin-Botton A, Honore C, Ahnfelt-Ronne J, Hecksher-Sorensen J, Ravassard P, Madsen OD, Rescan C, Frogne T: The EndoC-betaH1 cell line is a valid model of human beta cells and applicable for screenings to identify novel drug target candidates. Mol Metab 2018;8:144-157
24. Ravassard P, Hazhouz Y, Pechberty S, Bricout-Neveu E, Armanet M, Czernichow P, Scharfmann R: A genetically engineered human pancreatic beta cell line exhibiting glucose-inducible insulin secretion. J Clin Invest 2011;121:3589-3597
25. Carlotti F, Bazuine M, Kekarainen T, Seppen J, Pognonec P, Maassen JA, Hoeben RC: Lentiviral vectors efficiently transduce quiescent mature 3T3-L1 adipocytes. Mol Ther 2004;9:209-217
26. Back NK, Nijhuis M, Keulen W, Boucher CA, Oude Essink BO, van Kuilenburg AB, van Gennip AH, Berkhout B: Reduced replication of 3TC-resistant HIV-1 variants in primary cells due to a processivity defect of the reverse transcriptase enzyme. EMBO J 1996;15:4040-4049
27. Ricordi C, Socci C, Davalli AM, Staudacher C, Vertova A, Baro P, Sassi I, Braghi S, Guizzi N, Pozza G, et al.: Application of the automated method to islet isolation in swine. Transplant Proc 1990;22:784-785
28. Kozomara A, Birgaoanu M, Griffiths-Jones S: miRBase: from microRNA sequences to function. Nucleic Acids Res 2019;47:D155-D162
29. Li JH, Liu S, Zhou H, Qu LH, Yang JH: starBase v2.0: decoding miRNA-ceRNA, miRNA-ncRNA and protein-RNA interaction networks from large-scale CLIP-Seq data. Nucleic Acids Res 2014;42:D92-97
30. Hearn A, York IA, Rock KL: The specificity of trimming of MHC class I-presented peptides in the endoplasmic reticulum. J Immunol 2009;183:5526-5536
31. Eizirik DL, Colli ML, Ortis F: The role of inflammation in insulitis and beta-cell loss in type 1 diabetes. Nat Rev Endocrinol 2009;5:219-226
32. Gonzalez-Duque S, Azoury ME, Colli ML, Afonso G, Turatsinze JV, Nigi L, Lalanne AI, Sebastiani G, Carre A, Pinto S, Culina S, Corcos N, Bugliani M, Marchetti P, Armanet M, Diedisheim M, Kyewski B, Steinmetz LM, Buus S, You S, Dubois-Laforgue D, Larger E, Beressi JP, Bruno G, Dotta F, Scharfmann R, Eizirik DL, Verdier Y, Vinh J, Mallone R: Conventional and Neo-Antigenic Peptides Presented by beta Cells Are Targeted by Circulating Naive CD8+ T Cells in Type 1 Diabetic and Healthy Donors. Cell Metab 2018;

33. Thomaidou S, Zaldumbide A, Roep BO: Islet stress, degradation and autoimmunity. Diabetes Obes Metab 2018;20 Suppl 2:88-94
34. Oleson BJ, McGraw JA, Broniowska KA, Annamalai M, Chen J, Bushkofsky JR, Davis DB, Corbett JA, Mathews CE: Distinct differences in the responses of the human pancreatic beta-cell line EndoC-betaH1 and human islets to proinflammatory cytokines. Am J Physiol Regul Integr Comp Physiol 2015;309:R525-534
35. Hattori A, Matsumoto K, Mizutani S, Tsujimoto M: Genomic organization of the human adipocyte-derived leucine aminopeptidase gene and its relationship to the placental leucine aminopeptidase/oxytocinase gene. J Biochem 2001;130:235-241
36. Compagnone M, Cifaldi L, Fruci D: Regulation of ERAP1 and ERAP2 genes and their disfunction in human cancer. Hum Immunol 2019;80:318-324
37. Klein D, Misawa R, Bravo-Egana V, Vargas N, Rosero S, Piroso J, Ichii H, Umland O, Zhijie J, Tsinoremas N, Ricordi C, Inverardi L, Dominguez-Bendala J, Pastori RL: MicroRNA expression in alpha and beta cells of human pancreatic islets. PLoS One 2013;8:e55064
38. Sethupathy P, Corda B, Hatzigeorgiou AG: TarBase: A comprehensive database of experimentally supported animal microRNA targets. RNA 2006;12:192-197
39. Hong K, Xu G, Grayson TB, Shalev A: Cytokines Regulate beta-Cell Thioredoxin-interacting Protein (TXNIP) via Distinct Mechanisms and Pathways. J Biol Chem 2016;291:8428-8439
40. Kracht M.J.L. dEJP, Hoeben R.C., Roep B.O. and Zaldumbide A.: Bioluminescent reporter assay for monitoring ER stress in human beta cells. SC Rep 2018;
41. Beninga J, Rock KL, Goldberg AL: Interferon-gamma can stimulate post-proteasomal trimming of the N terminus of an antigenic peptide by inducing leucine aminopeptidase. J Biol Chem 1998;273:18734-18742
42. Urban S, Textoris-Taube K, Reimann B, Janek K, Dannenberg T, Ebstein F, Seifert C, Zhao F, Kessler JH, Halenius A, Henklein P, Paschke J, Cadel S, Bernhard H, Ossendorp F, Foulon T, Schadendorf D, Paschen A, Seifert U: The efficiency of human cytomegalovirus pp65(495-503) CD8+ T cell epitope generation is determined by the balanced activities of cytosolic and endoplasmic reticulum-resident peptidases. J Immunol 2012;189:529-538
43. Guasp P, Lorente E, Martin-Esteban A, Barnea E, Romania P, Fruci D, Kuiper JJW, Admon A, Lopez de Castro JA: Redundancy and Complementarity between ERAP1 and ERAP2 Revealed by their Effects on the Behcet's Disease-associated HLA-B*51 Peptidome. Mol Cell Proteomics 2019;18:1491-1510
44. Saveanu L, Carroll O, Lindo V, Del Val M, Lopez D, Lepelletier Y, Greer F, Schomburg L, Fruci D, Niedermann G, van Endert PM: Concerted peptide trimming by human ERAP1 and ERAP2 aminopeptidase complexes in the endoplasmic reticulum. Nat Immunol 2005;6:689-697
45. York IA, Chang SC, Saric T, Keys JA, Favreau JM, Goldberg AL, Rock KL: The ER aminopeptidase ERAP1 enhances or limits antigen presentation by trimming epitopes to 8-9 residues. Nat Immunol 2002;3:1177-1184
46. Saric T, Chang SC, Hattori A, York IA, Markant S, Rock KL, Tsujimoto M, Goldberg AL: An IFN-gamma-induced aminopeptidase in the ER, ERAP1, trims precursors to MHC class I-presented peptides. Nat Immunol 2002;3:1169-1176
47. LaPierre MP, Stoffel M: MicroRNAs as stress regulators in pancreatic beta cells and diabetes. Mol Metab 2017;6:1010-1023
48. Dong D, Fu N, Yang P: MiR-17 Downregulation by High Glucose Stabilizes Thioredoxin-Interacting Protein and Removes Thioredoxin Inhibition on ASK1 Leading to Apoptosis. Toxicol Sci 2016;150:84-96
49. Oslowski CM, Hara T, O'Sullivan-Murphy B, Kanekura K, Lu S, Hara M, Ishigaki S, Zhu LJ, Hayashi E, Hui ST, Greiner D, Kaufman RJ, Bortell R, Urano F: Thioredoxin-interacting protein mediates ER stress-induced beta cell death through initiation of the inflammasome. Cell Metab 2012;16:265-273

50. Morita S, Villalta SA, Feldman HC, Register AC, Rosenthal W, Hoffmann-Petersen IT, Mehdizadeh M, Ghosh R, Wang L, Colon-Negron K, Meza-Acevedo R, Backes BJ, Maly DJ, Bluestone JA, Papa FR: Targeting ABL-IRE1alpha Signaling Spares ER-Stressed Pancreatic beta Cells to Reverse Autoimmune Diabetes. Cell Metab 2017;25:883-897 e888

Table 1: Putative miRNA regulating ERAP1. ERAP1-miRNA motif and the energy folding characteristic of the miR-17 family on the ERAP1 UTR region. Data presented are according to in silico predictions performed on https://cm.jefferson.edu/rna22/Interactive/RNA22Controller.

miRNA	ERAP1-target motif	Folding energy (Kcal/mol)
Hsa-miR-20b-5p	CAAAGUGCUCAUAGUGCAGGUAG	-16.20
Hsa-miR-20a-5p	UAAAGUGCUUAUAGUGCAGGUAG	-16.20
Hsa-miR-106a-5p	AAAAGUGCUUACAGUGCAGGUAG	-16.00
Hsa-miR-17-5p	CAAAGUGCUUACAGUGCAGGUAG	-16.00
Hsa-miR-93-5p	CAAAGUGCUGUUCGUGCAGGUAG	-14.30
Hsa-miR-106b-5p	UAAAGUGCUGACAGUGCAGAU	-15.50

FIGURE LEGENDS

Figure 1. ERAP1 downregulation in surrogate beta cells reduce specific CTL activation. A) Amino acids sequence of the preproinsulin (PPI) signal peptide. The PPI signal peptide epitope sequence PPI_{15-24} is presented in between arrows. The target sequence for ERAP1 hydrophobic region is underlined. The N-term part of the proinsulin molecule is depicted as broken grey box. (n=3) (B) Insulin gene expression level in HEK 293T cells (white dots) and HEK 293T cells transduced with LV-CMV-PPI-bc-GFP (black dots) by qPCR (MOI=1). (n=3)-(C, D) ERAP1 and ERAP2 gene expression evaluated by qPCR in HEK 293T-PPI cells 4 days post-transduction with non-targeted shRNA lentiviruses (shNS), or ERAP1 specific shRNA (shERAP1). Gene expression levels are corrected for GAPDH used as housekeeping gene and presented as induction ratio (control set to 1). (n=3)- (E) Insulin protein expression in shERAP1 and shNS modified cells assessed by flow cytometry. HEK 293T were used as a negative control. (F) HLA class I surface expression of shNS and shERAP1 modified cells presented as Mean Fluorescence PE intensity (n=6) (G) CD107a surface expression on CD8 positive cells after coculture with the modified HEK 293T cells. Data are presented as percentage decrease to control set at 100% (n=3). (H) MIP1β secretion of PPI_{15-24} specific CTLs after a 2 hours co-culture with 293T-PPI-shNS or shERAP1 (n=3).

Figure 2. Transcriptional and post-transcriptional regulation of ERAP1. A) XBP1 spliced isoform expression and (B) ERAP1 gene expression in EndoC-βH1 cells after 24h treatment with proinflammatory cytokines (IFNγ, IL-1β) (light grey dots) or thapsigargin (dark grey dots), as determined by qPCR. Gene expression levels are corrected for GAPDH used as housekeeping gene and presented as induction ratio (non-treated controls set to 1). (n=4)- (C) ERAP1 protein expression level determined by western blot analysis of EndoC-βH1 treated with proinflammatory cytokines (IFNγ, IL-1β) or thapsigargin. Actin was used as internal control for quantification (unprocessed image and quantification n=3 are presented in supplementary figure 4). (D) Luciferase activity measured in EndoC-βH1 cells transfected with the ERAP1 promoter reporter construct after treatment with cytokines or thapsigargin for 24h (n=8). Luciferase was measured in relative light units (RLU) and presented as relative induction ratio (Luciferase activity in absence of treatment was arbitrarily set to 1). (E) Venn diagram showing the overlap between miRNAs found in beta cells and predicted ERAP1 targeting miRNAs according to miRbase V21.0 and TarBase V8 (upper panel). Schematic representation of the miR-17 targeting sequence in the 3'-UTR of ERAP1 mRNA (wt 3'-UTR) and the mutated ERAP1 UTR (mut 3'-UTR, mutations shown in red) in the luciferase reporter constructs with the predicted folding energy (lower panel). (F) Relative luciferase activity after co-

transfection of miR-ns (negative control) or miR-17 with ERAP1 wt UTR luciferase construct or ERAP1 mut UTR in HEK 293T cells (n=3). Data are presented as induction ratio (control miR-ns set to 1). (G) ERAP1 and (H) Insulin gene expression in EndoC-βH1 cell transfected with miR-ns, miR-17 and anti-miR-17, analyzed by qPCR, 24 hours post-transfection (n=3). (I) Relative expression of miR-17 in EndoC-βH1 cells after IFNγ and IL-1β stimulation compared to non-treated cells (n=3). (J) Relative expression of ERAP1 and (K) Insulin in EndoC-βH1 cells following miR-17 or control miR-ns transfection in the presence or absence of cytokine stimulation (n=5). Gene expression levels are corrected for GAPDH used as housekeeping gene. miRNA expression is corrected for RNU6 expression used as control. All data are presented as induction ratio (controls set to 1).

Figure 3. miR-17 and ERAP1 regulation by IRE1α inhibition. A) miR-17 expression and B) ERAP1 gene expression in EndoC-βH1 cells after 6 hours treatment with IFNγ and IL-1β, in the presence or absence of the IRE1α inhibitor MKC3946 (10uM), as determined by qPCR. (C, D) miR-17 expression and ERAP1 gene after 24 hours of treatment (n=3). (E) XBP1 spliced isoform and (F) ERAP1 gene expression in EndoC-βH1 cells after 24 hours of cytokines treatment in the presence of increasing amounts of MKC3946 (10, 20 and 50 uM). Gene expression levels are corrected for GAPDH used as housekeeping gene (n=3). Data are presented as induction ratio compared to expression level in non-treated cells used as control.

Figure 4. IRE1α regulates ERAP1 expression and PPI_{15-24} presentation in human islets. A) XBP1 spliced isoform and (B) ERAP1 gene expression, measured by qPCR, in intact human islets treated with after 24h treatment with cytokines (light grey dots) or thapsigargin (dark grey dots), in the presence or absence of MKC3946 (10uM) Gene expression levels are corrected for GAPDH used as housekeeping gene. All data are presented as induction ration (controls set to 1). (n=3) (C) Flowchart of the islet cells/PPI_{15-24} specific CTLs co-culture experiment. (D) HLA class I expression in dispersed islets, upon 24 hours cytokines treatment, in the presence or absence of MKC3946. (E) CD107a surface expression and (F) MIP1β secretion of PPI_{15-24} specific CTLs after a 2 hours co-culture with HLA-A2 positive dispersed islets. Data were collected from replicates of three different donors (color-coded). (G) Schematic representation of the working model for post-transcriptional ERAP1 regulation and PPI_{15-24} processing via IRE1α-regulated miR-17.

Figure 1

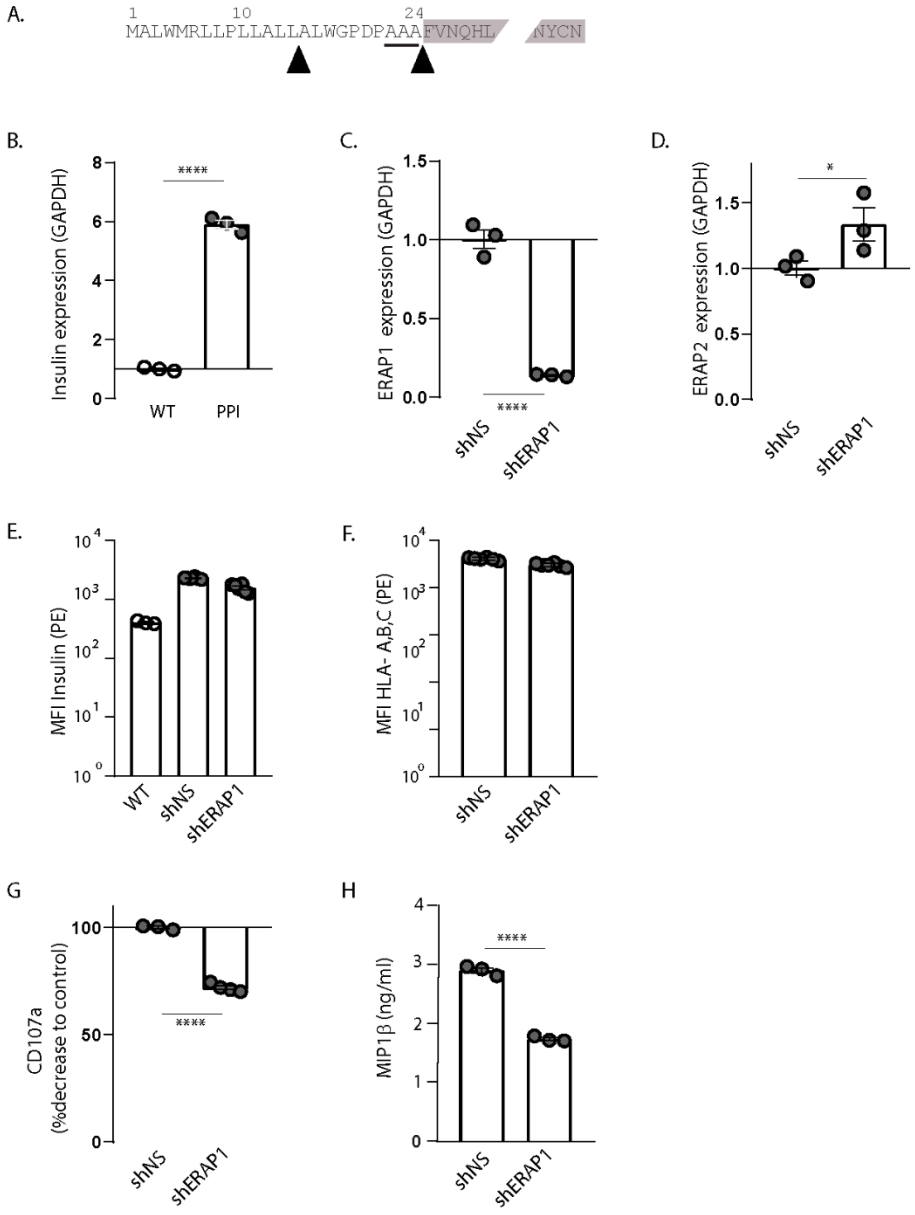
A.
1
10
24
MALWMRLLPLLALLALWGPDPAAAFVNQHL
NYCN
B.
Insulin expression (GAPDH)
****
WT
PPI
C.
ERAP1 expression (GAPDH)
****
shNS
shERAP1
D.
ERAP2 expression (GAPDH)
*
shNS
shERAP1
E.
MFI Insulin (PE)
WT
shNS
shERAP1
F.
MFI HLA- A,B,C (PE)
shNS
shERAP1
G
CD107a
(%decrease to control)
****
shNS
shERAP1
H
MIP1β (ng/ml)
****
shNS
shERAP1

Figure 2

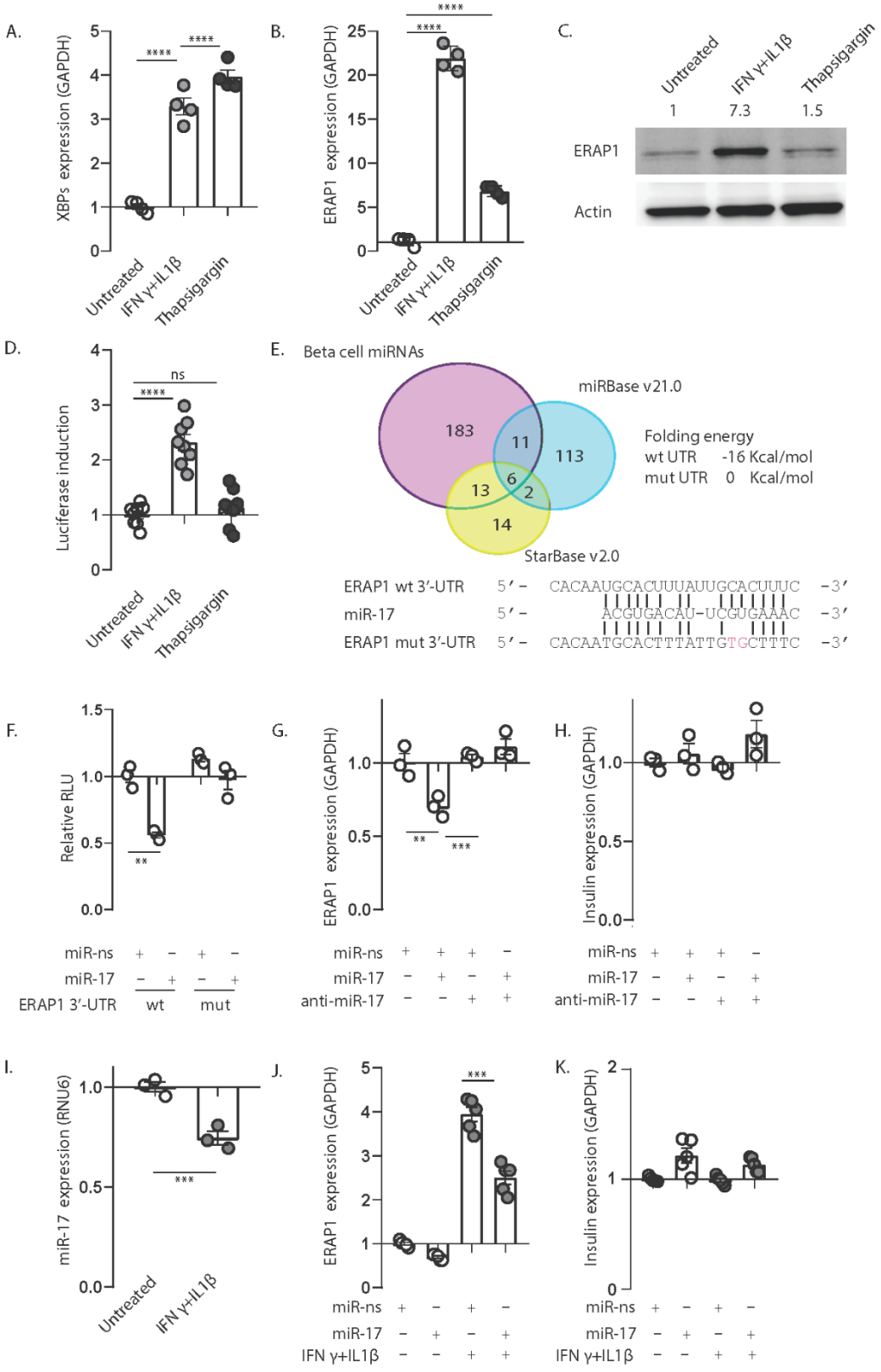
A.
XBPs expression (GAPDH)
Untreated
IFN γ+IL1β
Thapsigargin
B.
ERAP1 expression (GAPDH)
C.
Untreated
IFN γ+IL1β
Thapsigargin
1
7.3
1.5
ERAP1
Actin
D.
Luciferase induction
ns
E.
Beta cell miRNAs
miRBase v21.0
183
11
113
6
13
2
14
StarBase v2.0
Folding energy
wt UTR -16 Kcal/mol
mut UTR 0 Kcal/mol
ERAP1 wt 3′-UTR 5′- CACAAUGCACUUUAUUGCACUUUC -3′
miR-17 5′- ACGUGACAU-UCGUGAAAC -3′
ERAP1 mut 3′-UTR 5′- CACAATGCACTTTATTGTGCTTTC -3′
F.
Relative RLU
miR-ns
miR-17
ERAP1 3′-UTR
wt
mut
G.
ERAP1 expression (GAPDH)
anti-miR-17
H.
Insulin expression (GAPDH)
I.
miR-17 expression (RNU6)
J.
IFN γ+IL1β
K.

Figure 3

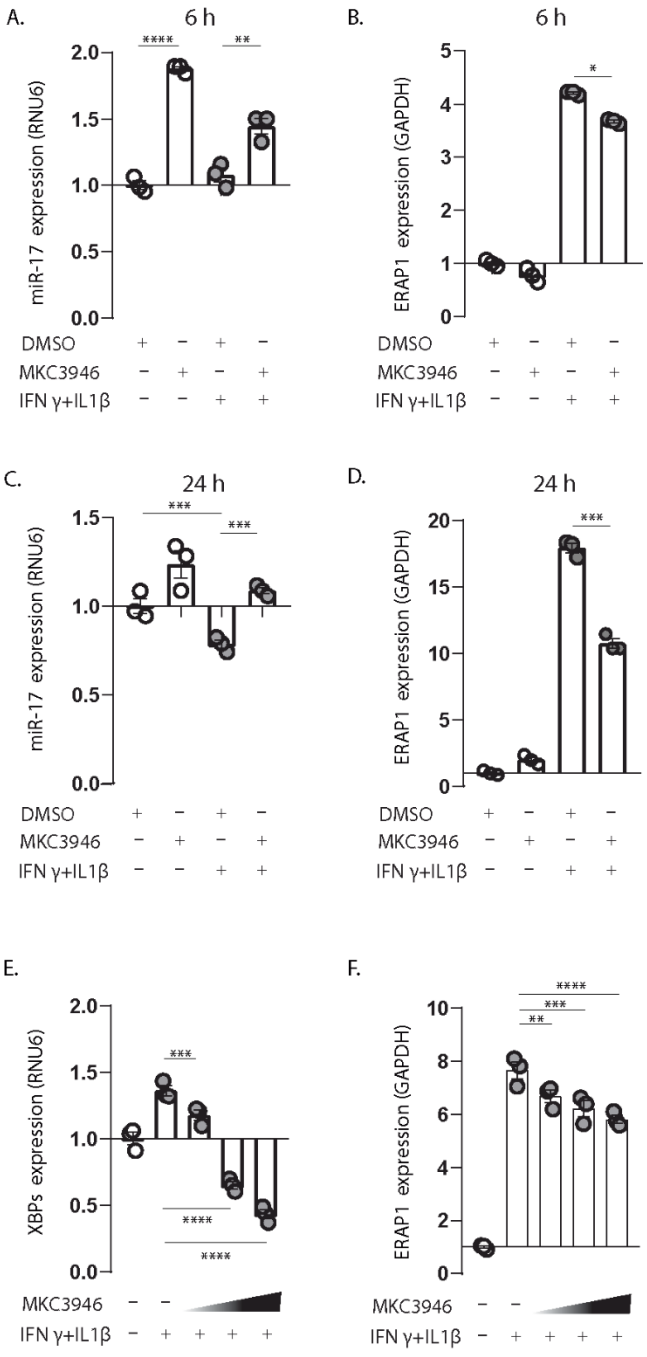
A.
6 h
miR-17 expression (RNU6)
DMSO
MKC3946
IFN γ+IL1β
B.
6 h
ERAP1 expression (GAPDH)
C.
24 h
D.
24 h
E.
XBPs expression (RNU6)
F.
ERAP1 expression (GAPDH)

Figure 4

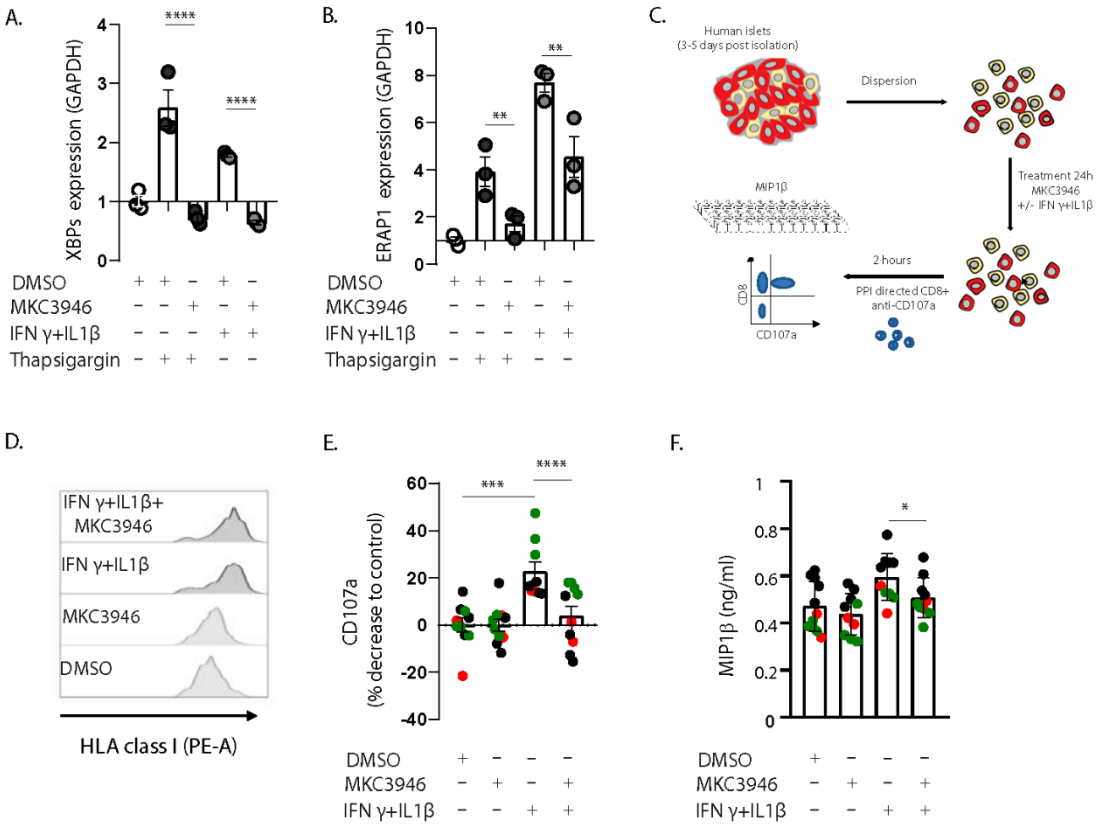
A.
XBPs expression (GAPDH)
****
****
DMSO
MKC3946
IFN γ+IL1β
Thapsigargin
B.
ERAP1 expression (GAPDH)
**
**
DMSO
MKC3946
IFN γ+IL1β
Thapsigargin
C.
Human islets
(3-5 days post isolation)
Dispersion
Treatment 24h
MKC3946
+/- IFN γ+IL1β
MIP1β
2 hours
PPI directed CD8+
anti-CD107a
CD8
CD107a
D.
IFN γ+IL1β+
MKC3946
IFN γ+IL1β
MKC3946
DMSO
HLA class I (PE-A)
E.
CD107a
(% decrease to control)
***
****
DMSO
MKC3946
IFN γ+IL1β
F.
MIP1β (ng/ml)
*
DMSO
MKC3946
IFN γ+IL1β

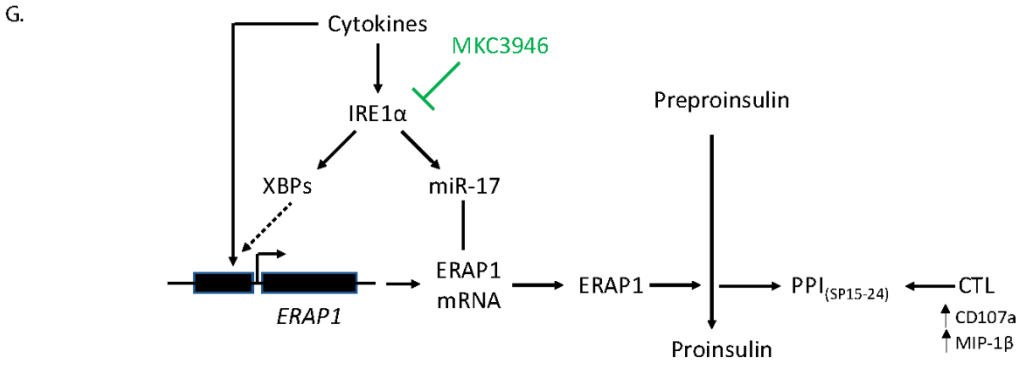
G.
Cytokines
MKC3946
IRE1α
XBPs
miR-17
ERAP1
mRNA
ERAP1
Preproinsulin
PPI(SP15-24)
CTL
CD107a
MIP-1β
Proinsulin

Supplementary Figure S1

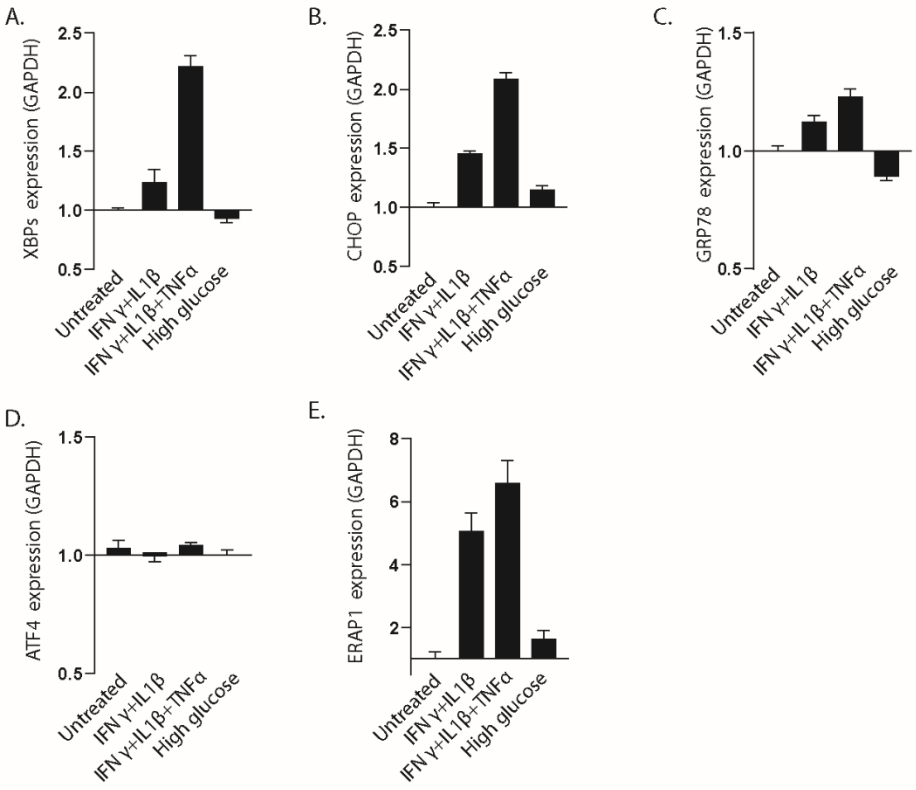

Supplementary Figure S2

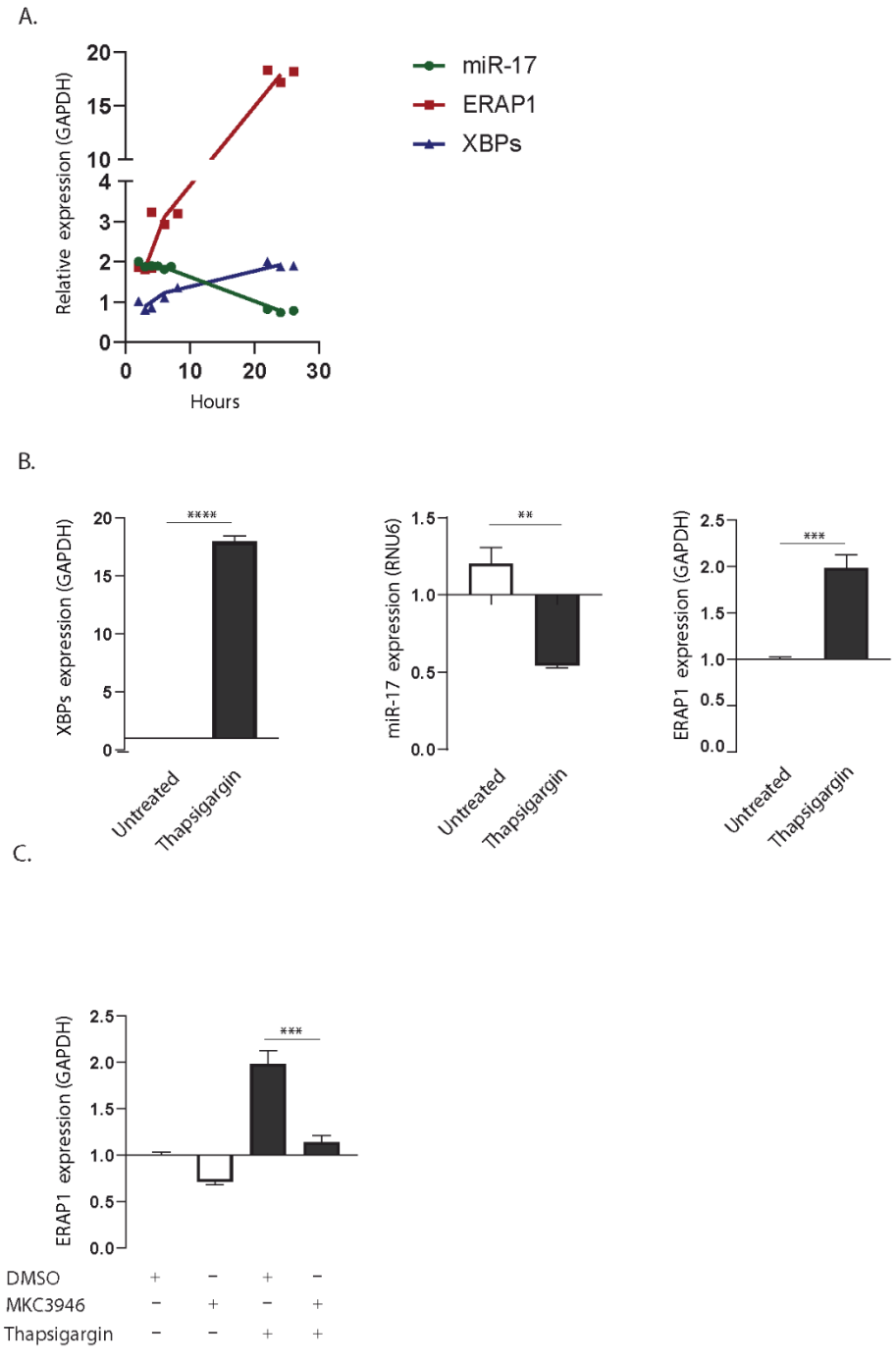

Supplementary Figure S3

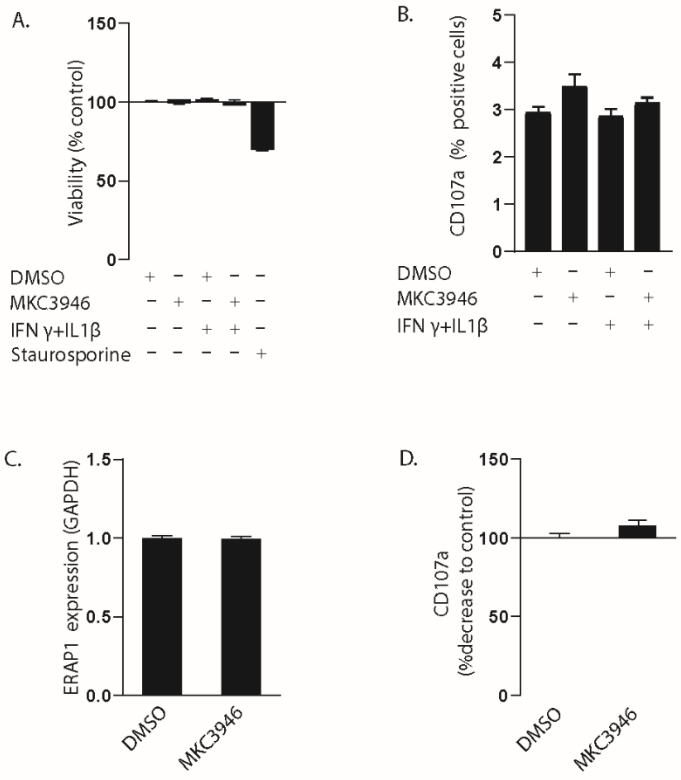

Supplementary Figure S4

A.

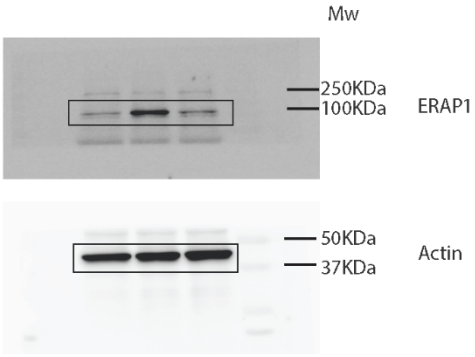

B.

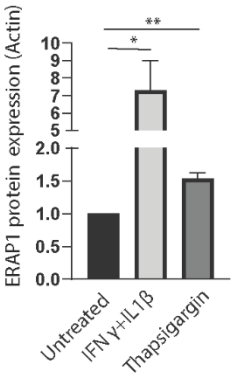

Supplementary Table 1: ERAP1 regulation by miRNAs. Most highly expressed Beta cell specific miRNAs (cut-off CT30) (33) (left column). ERAP1 targeted miRNAs predicted by miRbase v21.0 (middle column) and Tarbase v.8 (right column). Overlapping miRNAs presented in table 1 and figure 2E are highlighted in yellow.

Beta cell miRNAs* **(Lowering CT values)**	*miRDB predicted ERAP1 miRNAs (Lowering target score)*	*TarBase v.8 predicted ERAP1 miRNAs (Lowering prediction score)*
hsa-miR-192-3p	*hsa-miR-3646*	*hsa-miR-20a-5p*
hsa-miR-146a-5p	*hsa-miR-7515*	*hsa-miR-126-5p*
hsa-miR-192-5p	*hsa-miR-1253*	*hsa-miR-106b-5p*
hsa-miR-708-5p	*hsa-miR-16-2-3p*	*hsa-miR-106a-5p*
hsa-miR-181-5p	*hsa-miR-195-3p*	*hsa-miR-374a-5p*
hsa-miR-194-5p	*hsa-miR-4703-5p*	*hsa-let-7f-1-3p*
hsa-miR-221-3p	*hsa-miR-3942-5p*	*hsa-miR-140-3p*
hsa-miR-532-5p	*hsa-miR-568*	*hsa-miR-29b-3p*
hsa-miR-500	*hsa-miR-3662*	*hsa-miR-29c-3p*
hsa-miR-20b-5p	*hsa-miR-106b-5p*	*hsa-miR-29a-3p*
hsa-miR-222-3p	*hsa-miR-20a-5p*	*hsa-miR-31-3p*
hsa-miR-455-5p	*hsa-miR-20b-5p*	*hsa-miR-5690*
hsa-miR-20a-5p	*hsa-miR-106a-5p*	*hsa-miR-3653-3p*
hsa-miR-532-3p	*hsa-miR-17-5p*	*hsa-miR-93-5p*
hsa-miR-106a-5p	*hsa-miR-30e-3p*	*hsa-miR-28-5p*
hsa-miR-17-5p	*hsa-miR-30d-3p*	*hsa-miR-20b-5p*
hsa-miR-660-5p	*hsa-miR-30a-3p*	*hsa-miR-2110*
hsa-miR-133a	*hsa-miR-3688-5p*	*hsa-miR-193a-5p*
hsa-miR-886-3p	*hsa-miR-98-3p*	*hsa-miR-17-5p*
hsa-miR-874	*hsa-miR-93-5p*	*hsa-miR-361-5p*
hsa-miR-222-5p	*hsa-miR-519d-3p*	*hsa-miR-3605-5p*
hsa-miR-455-3p	*hsa-miR-526b-3p*	*hsa-miR-522-5p*
hsa-miR-15b-5p	*hsa-miR-513a-5p*	*hsa-miR-523-3p*
hsa-miR-93-5p	*hsa-miR-6073*	*hsa-miR-124-5p*
hsa-miR-19a-3p	*hsa-miR-3529-3p*	*hsa-miR-1-3p*
hsa-miR-886-5p	*hsa-miR-6770-5p*	*hsa-miR-23b-3p*
hsa-miR-142-3p	*hsa-miR-6864-5p*	*hsa-miR-210-3p*
hsa-miR-151-3p	*hsa-miR-205-3p*	*hsa-miR-147a*
hsa-miR-565	*hsa-miR-138-2-3p*	*hsa-miR-129-2-3p*
hsa-miR-223-3p	*hsa-miR-4316*	*hsa-miR-21-3p*
hsa-miR-153-3p	*hsa-miR-4534*	*hsa-miR-26b-5p*
hsa-miR-140-5p	*hsa-miR-608*	*hsa-miR-335-5p*
hsa-miR-520c-3p	*hsa-miR-3163*	*hsa-miR-146a-5p*
hsa-miR-425-5p	*hsa-miR-4666a-3p*	*hsa-miR-27a-3p*
hsa-miR-768-3p	*hsa-miR-4651*	*hsa-miR-122-5p*
hsa-miR-338-3p	*hsa-miR-203a-3p*	
hsa-miR-130a-3p	*hsa-miR-5584-5p*	
	hsa-let-7b-3p	
	hsa-let-7f-1-3p	
	hsa-let-7a-3p	
	hsa-miR-3065-5p	
	hsa-miR-129-5p	

hsa-miR-339-5p	*hsa-miR-7159-5p*	
hsa-miR-125a-3p	*hsa-miR-579-3p*	
hsa-miR-126-3p	*hsa-miR-95-5p*	
hsa-miR-19b-3p	*hsa-miR-3154*	
hsa-miR-135a-5p	*hsa-miR-519a-3p*	
hsa-miR-146b-5p	*hsa-miR-519c-3p*	
hsa-miR-28-5p	*hsa-miR-519b-3p*	
hsa-miR-26b-3p	*hsa-miR-335-3p*	
hsa-miR-378-3p	*hsa-miR-219a-1-3p*	
hsa-miR-769-5p	*hsa-miR-6501-3p*	
hsa-miR-106b-5p	*hsa-miR-1910-3p*	
hsa-miR-877-5p	*hsa-miR-6511a-5p*	
hsa-miR-572	*hsa-miR-668-3p*	
hsa-miR-766-3p	*hsa-miR-6839-3p*	
hsa-miR-590-5p	*hsa-miR-6074*	
hsa-miR-28-3p	*hsa-miR-6509-5p*	
hsa-miR-200a-5p	*hsa-miR-4729*	
hsa-miR-374a-5p	*hsa-miR-3911*	
hsa-miR-126-5p	*hsa-miR-30c-2-3p*	
hsa-miR-20a-3p	*hsa-miR-3926*	
hsa-miR-125a-5p	*hsa-miR-1-5p*	
hsa-miR-526b-3p	*hsa-miR-3144-3p*	
hsa-miR-135b-5p	*hsa-miR-30c-1-3p*	
hsa-miR-95-3p	*hsa-miR-887-5p*	
hsa-miR-597	*hsa-miR-1252-5p*	
hsa-miR-149-5p	*hsa-miR-8087*	
hsa-miR-375	*hsa-miR-8064*	
hsa-miR-642a-5p	*hsa-miR-548c-3p*	
hsa-miR-26b-5p	*hsa-miR-4517*	
hsa-miR-218-5p	*hsa-miR-4311*	
hsa-miR-138-1-3p	*hsa-miR-3121-3p*	
hsa-miR-200a-3p	*hsa-miR-4775*	
hsa-miR-30d-3p	*hsa-miR-580-5p*	
hsa-miR-195-5p	*hsa-miR-544a*	
hsa-miR-30c-5p	*hsa-miR-1185-1-3p*	
hsa-miR-200b-3p	*hsa-miR-1185-2-3p*	
hsa-miR-30b-5p	*hsa-miR-655-3p*	
hsa-miR-301a-3p	*hsa-miR-374c-5p*	
hsa-miR-150-5p	*hsa-let-7f-2-3p*	
hsa-miR-551b-3p	*hsa-miR-3160-5p*	
hsa-miR-328	*hsa-miR-6858-3p*	
hsa-miR-801	*hsa-miR-151a-5p*	
hsa-miR-193a-5p	*hsa-miR-151b*	
hsa-miR-744-5p	*hsa-miR-5704*	
	hsa-miR-153-5p	
	hsa-miR-4779	
	hsa-miR-664b-3p	
	hsa-miR-561-5p	
	hsa-miR-4790-3p	
	hsa-miR-888-5p	
	hsa-miR-299-5p	

hsa-miR-191-5p	*hsa-miR-369-3p*	
hsa-miR-429	*hsa-miR-1252-3p*	
hsa-let-7g-4	*hsa-miR-4461*	
hsa-miR-454-3p	*hsa-miR-450b-5p*	
hsa-miR-210	*hsa-miR-505-5p*	
hsa-miR-423-5p	*hsa-miR-1306-5p*	
hsa-miR-652-3p	*hsa-miR-3123*	
hsa-miR-141-3p	*hsa-miR-7-2-3p*	
hsa-miR-374b-5p	*hsa-miR-659-5p*	
hsa-miR-923	*hsa-miR-4693-3p*	
hsa-miR-92a-3p	*hsa-miR-7-1-3p*	
hsa-miR-197-3p	*hsa-miR-4516*	
hsa-miR-145-5p	*hsa-miR-5696*	
hsa-miR-128-3p	*hsa-miR-4716-5p*	
hsa-miR-26a-5p	*hsa-miR-656-3p*	
hsa-miR-137	*hsa-miR-627-5p*	
hsa-miR-99b-3p	*hsa-miR-7850-5p*	
hsa-miR-93-3p	*hsa-miR-3121-5p*	
hsa-miR-99b-5p	*hsa-miR-3182*	
hsa-miR-760	*hsa-miR-208a-5p*	
hsa-miR-598	*hsa-miR-5692a*	
hsa-miR-143-3p	*hsa-miR-208b-5p*	
hsa-miR-342-3p	*hsa-miR-330-3p*	
hsa-miR-103a-3p	*hsa-miR-670-3p*	
hsa-miR-186-5p	*hsa-miR-31-5p*	
hsa-miR-340-3p	*hsa-miR-6824-5p*	
hsa-miR-7-5p	*hsa-miR-300*	
hsa-miR-212-3p	*hsa-miR-381-3p*	
hsa-miR-30e-5p	*hsa-miR-4282*	
hsa-miR-425-3p	*hsa-miR-629-5p*	
hsa-miR-340-5p	*hsa-miR-4694-3p*	
hsa-miR-320a	*hsa-miR-3653-3p*	
hsa-miR-301b-3p	*hsa-miR-363-5p*	
hsa-miR-339-3p	*hsa-miR-944*	
hsa-miR-365a-3p	*hsa-miR-6745*	
hsa-miR-671-3p	*hsa-miR-6737-5p*	
hsa-miR-29a-3p	*hsa-miR-6819-5p*	
hsa-miR-29b-3p	*hsa-miR-421*	
hsa-miR-324-3p	*hsa-miR-6812-5p*	
hsa-miR-625-3p		
hsa-let-7d-4		
hsa-miR-34a-3p		
hsa-miR-29a-5p		
hsa-miR-101-3p		

hsa-miR-484		
hsa-miR-30d-5p		
hsa-miR-16-5p		
hsa-miR-7-2-3p		
hsa-miR-30e-3p		
hsa-miR-200c-3p		
hsa-miR-132-3p		
hsa-miR-30a-5p		
hsa-miR-335-5p		
hsa-miR-7-1-3p		
hsa-miR-203a-3p		
hsa-miR-27a-3p		
hsa-miR-148b-3p		
hsa-miR-296-5p		
hsa-miR-25-3p		
hsa-miR-193b-3p		
hsa-miR-34a-5p		
hsa-miR-200b-5p		
hsa-miR-135a-3p		
hsa-let-7e-4		
hsa-miR-361-5p		
hsa-miR-628-5p		
hsa-miR-331-3p		
hsa-miR-21-5p		
hsa-miR-184		
hsa-miR-185-5p		
hsa-miR-29c-5p		
hsa-miR-129-3p		
hsa-let-7a-5p		
hsa-miR-324-5p		
hsa-let-7b-5p		
hsa-miR-29c-3p		
hsa-miR-22-5p		
hsa-miR-655-3p		
hsa-miR-130b-3p		
hsa-miR-369-3p		
hsa-miR-574-3p		
hsa-miR-380-5p		
hsa-miR-24-3p		
hsa-miR-139-5p		
hsa-miR-654-3p		
hsa-miR-134		
hsa-miR-27b-3p		
hsa-miR-491-5p		